SEMARAK ILMU PUBLISHING

Journal of Advanced Research in Fluid Mechanics and Thermal Sciences

Journal homepage:
https://semarakilmu.com.my/journals/index.php/fluid_mechanics_thermal_sciences/index
ISSN: 2811-3950

Computational Modelling of the Aerodynamic Noise of the Full-Scale Pantograph of High-Speed Trains

Ahmed Farouk AbdelGawad[1], Naser Mohammed Aljameel[1], Ramy Elsayed Shaltout[1,2,*]

[1] Mechanical Power Engineering Dept., Faculty of Engineering, Zagazig University, Zagazig 44519, Egypt
[2] Civil Engineering Department, Faculty of Engineering and Material Sciences, German University in Cairo, 11835, Egypt

ARTICLE INFO

Article history:
Received 26 September 2021
Received in revised form 8 January 2022
Accepted 11 January 2022
Available online 6 March 2022

Keywords:
High speed train; Pantograph aerodynamics; Computational aeroacoustics; Computational fluid dynamics; Aerodynamic noise

ABSTRACT

High speed rail systems have significantly developed due to the increased demand on the rail transportation in the recent years. The necessity for enhancing the environmental sustainability of the rail systems imposed many challenges for the researchers to decrease the level of noise generated by the high speed rail systems. This paper aims to investigate the aerodynamic noise of the pantograph of the high-speed trains in different operating conditions. Computational fluid dynamics technique was used to assess the acoustic noise of the pantograph components. Three-dimensional computational simulations were performed using FLUENT software. Comprehensive analyses of the acoustic pressure and the air velocity distributions were accomplished for the detailed full-scale pantograph components. A modified model for the pantograph was introduced to reduce the aerodynamic noise of the pantograph's panhead. Good agreement was found between the obtained results and the reported results in the literature. Different design profile for the collector was then presented as a possible solution for the reduction of both the aerodynamic noise and the reduction of the fluctuating forces at the panhead-catenary interaction, which affects the quality of the power transmitted to the high-speed train. Vortex shedding was the main source of noise at the pantograph panhead and knee. Based on the obtained computational results, it was found that the use of an elliptic-edge cross-section bars can be a potential modification in the collector shape that can reduce the aerodynamic noise at the panhead.

1. Introduction

Due to the large expansion in the transportation systems around the world, the use of high-speed trains (HST) has been significantly developed in the last 50 years. Important measures have been taken to improve the environmental sustainability of high-speed rail systems. One of the most important measures is the noise mitigation, which improves the impact of the HST on the environment [1]. Thus, it is crucial for all HST operators and infrastructure managers to determine the main sources of noise.

* *Corresponding author.*
E-mail address: ramy.shaltout@guc.edu.eg

https://doi.org/10.37934/arfmts.93.1.94109

These sources of noise in high-speed systems include: the aerodynamic noise, the turbulent boundary layer (TBL) noise, the rolling noise, the equipment noise, car interspacing noise and traction noise [2-4,46]. However, for the high-speed rail systems, especially above 250 km/h, the dominant sources of noise are the wheel/rail interaction (rolling) noise and the aerodynamic noise [2,5].

The influence of the aerodynamic noise is notable for velocities above 220 km/h. For velocities above 350 km/h, it was noticed that the noise from train aerodynamic becomes considerable compared with the rolling noise [2]. At train speed of 370 km/h, the aerodynamic noise contribution becomes higher than the rolling contact noise contribution in the global pass-by noise [1,2]. The aerodynamic noise mainly comes from the aeroacoustics sources, namely: the pantograph and the TBL [6]. When dealing with aeroacoustics in HST, two phenomena should be considered: the first, is the generated noise by the air flow around train structure elements, which might include the cavity and vortex shedding noises; the second, is the turbulent flow noise [1]. Most of the research works in the literature only focus on the vibration of the catenary caused by the impact of pantograph. The influence of the environmental perturbation was seldom considered [5].

Various studies have been reported to assess the aerodynamic performance of the pantograph of high-speed trains [7-9]. In fact, the noise of aeroacoustics from pantograph during high-speed operation has become one of the major sources of noise of any train, which must be decreased to meet standards of environment that limit road noise. Therefore, there is a strong demand to reduce aerodynamic noise of pantographs in order to reduce noise in the rail environment. Hence, continuous efforts, to achieve this goal, have led to the development of low-noise pantographs [47-50].

Poisson [5] reported that the pantograph noise was the main source of the aerodynamic noise for Shinkansen E2-1000 running at speed of 360 km/h. An experimental investigation was carried out by Nagakura [10] to determine the sources of noise in Shinkansen trains. Wind tunnel tests for a model of 1/5-scale train were compared to field noise measurements with acoustic mirror. It was found that the front pantograph noise was the most dominant source of noise. Lee *et al.,* [11] investigated experimentally the aerodynamic characteristics of KTX-II high-speed train pantograph system in a wind tunnel. They demonstrated an optimized pantograph panhead to enhance the aerodynamic drag and lift forces on the pantograph.

Wind tunnel experiments has been carried out to assess the pantograph aerodynamic performance [12-15]. Lölgen *et al.,* [12] carried out wind tunnel tests for a full-scale pantograph model at air speeds up to 400 km/h. They noticed that a strong noise, caused by vortex shedding, was detected from the strips presenting the contact of the pantograph with the catenary line. Lauterbach *et al.,* [14] performed an aeroacoustics wind tunnel tests to measure the weighted sound pressure level (SPL) time history for 1/25-scale of ICE3 high-speed train model. They noted that, at frequencies above 5000 Hz for a 1/25-scale mock-up, the dominant noise is the pantograph noise. Recently, Noh [16] investigated experimentally the aeroacoustics noise generated by major parts of full-scale pantograph at different air speeds using wind tunnel tests. It was found that the pantograph panhead and the knee are the main sources of noise generated by the pantograph.

Due to the complexity of the pantograph system, field measurements were difficult to define the aerodynamic noise that comes from the pantograph components. Therefore, computational investigations have been carried out using CFD models to simulate the level of noise and determine the sound pressure spectrum of the high-speed pantograph system [17-20]. By using the results of the computational simulations, new designs and modifications can be performed on the pantograph to enhance the noise and sound exposure levels in high-speed train environment [7,20-23]. An empirical aerodynamic noise model was presented by Zhang [3]. Based on their model, the aerodynamic noise can be estimated by subtracting the rolling noise calculated by the indirect

roughness method (IRM), from the total measured pass-by noise. Xiao-Ming *et al.,* [24] computationally investigated the aeroacoustics behavior of the Faiveley CX-PG high-speed pantograph. They found that the vortex structure produced in the flow filed around the pantograph is the main dominating noise source especially at the pantograph insulator, upper and bottom frames, and the lower arm. They concluded that the aerodynamic noise can be reduced by the variation of the vortices shedding positions.

Based on the above literature survey, we conclude that to decrease the noise level of a pantograph, it is necessary to comprehend the mechanism of noise generation for a pantograph. But it is problematic to estimate this mechanism by analogy. Thus, the present work aims to investigate the aerodynamic performance of SSS87 pantograph and computationally assess the acoustic noise emissions of the pantograph at different operating conditions.

The obtained results were validated using the computational and experimental results reported in the literature. Further modifications on the pantograph panhead were investigated and the computational simulation of these modifications are presented.

2. Present Pantograph Model

All modern high-speed train networks around the world are electrified. The pantograph is the component which provides the rolling stock with the power transmitted through the catenary line. The dynamic interaction between the catenary and the pantograph has utmost importance to maintain a stable power transmission to the rolling stocks. Various studies have been carried out to simulate and investigate the characteristics of the pantograph-catenary interaction [25]. Most of current designs of the pantograph systems are scissors type except Shinkansen 500 series which has telescopic pantograph system [26]. In general, any of the existing pantograph topologies should provide three main functions: Panhead lifting to maintain contact with the catenary wire; dealing with the displacements caused by the passage of middle arms; managing the high-amplitude excitations caused at low frequencies during operation [27]. The pantograph consists of many complex sub-components which affects the aerodynamics of the pantograph.

The SSS87 pantograph model in this paper is the high-speed pantograph [28,29]. Figure 1 depicts a 3D model of the articulated frame of the pantograph that consists of: panhead; upper and lower arms; knee; and a coupling rod. The panhead represents the critical part influencing the aerodynamic performance in the high-speed pantograph system.

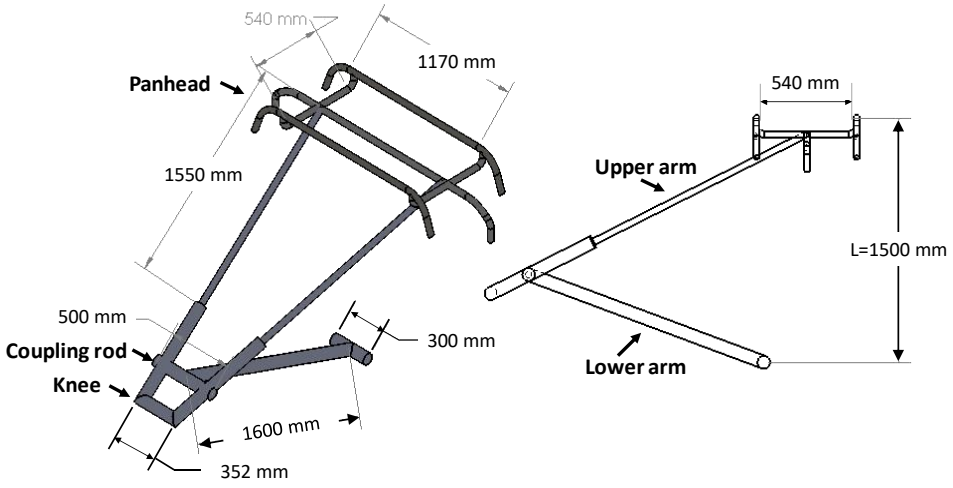

Fig. 1. Geometric description of SSS87 articulated pantograph

3. Computational Model Description

The proposed computational domain in this work was defined in FLUENT software package version 18.2. It has a cylindrical form with a diameter of 2L = 3 m and a length of 4L = 6 m. Where L = 1.5 m, which represents the characteristic length shown in Figure 1. As the SSS87 pantograph is symmetrical, a symmetry plan was introduced to consider only half the domain surrounding the pantograph in order to reduce the computational run-time as shown in Figure 2(a). The inlet condition to the domain was defined as the value of the air velocity without turbulent fluctuations. "Pressure outlet" condition was defined at the exit as seen in Figure 2(b).

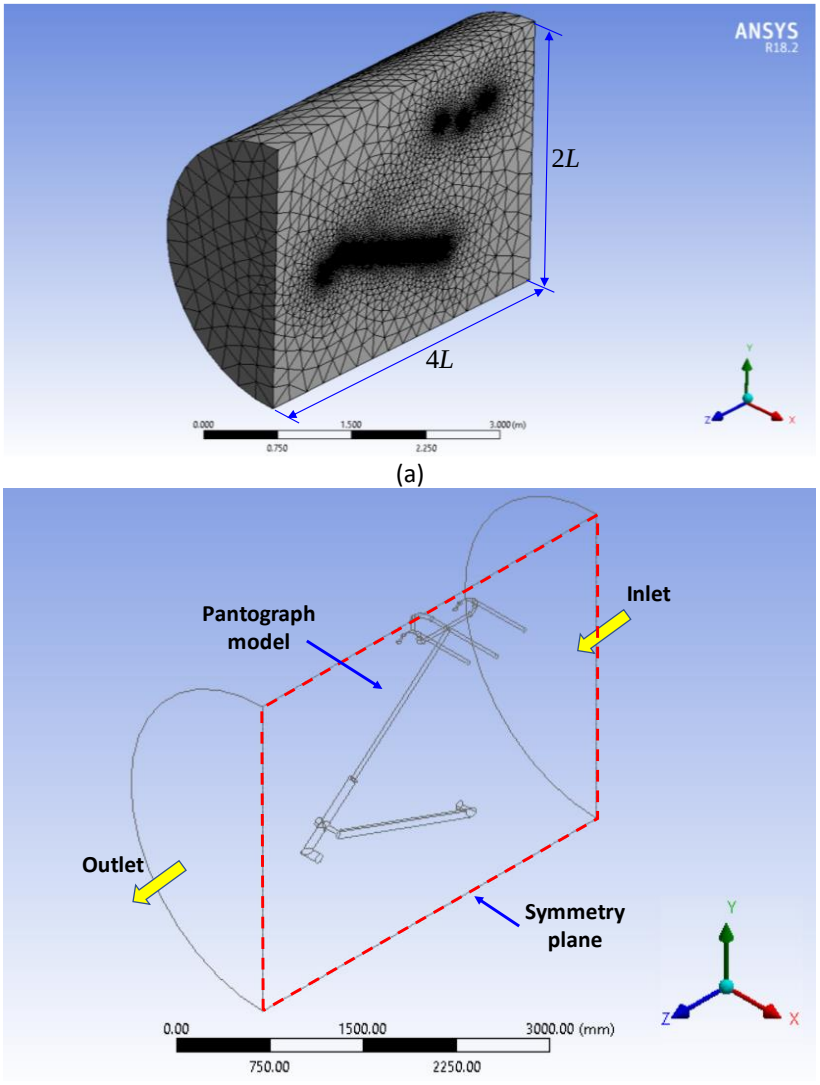

Fig. 2. Proposed computational domain

3.1 Mesh Sensitivity Analysis

Achieving a good accuracy of the simulation results depends mainly on the computational grid size. The element size in the grid should not exceed 1/5 of the flow wavelength considered. Mesh refinement was applied at the wall boundaries as well as the pantograph frame. Initially, an element size of 0.04 m was considered for the validation of the obtained results with the experimental and computational results in the literature [28,29].

Further refinement procedure was assumed to adopt the accuracy of the computational results. Thus, a mesh-element size of 0.00004 m was used for the simulation purposes in the present work. Figure 3 represents the variation of the maximum static pressure at the pantograph's panhead with grid size. The number of mesh elements that gives the accurate and best result is selected to be 1.34 million elements corresponding to the point highlighted in Figure 3. As can be seen in Figure 3, there is no change of the value of the static pressure with further increase of the number of grid elements above 1.34 million.

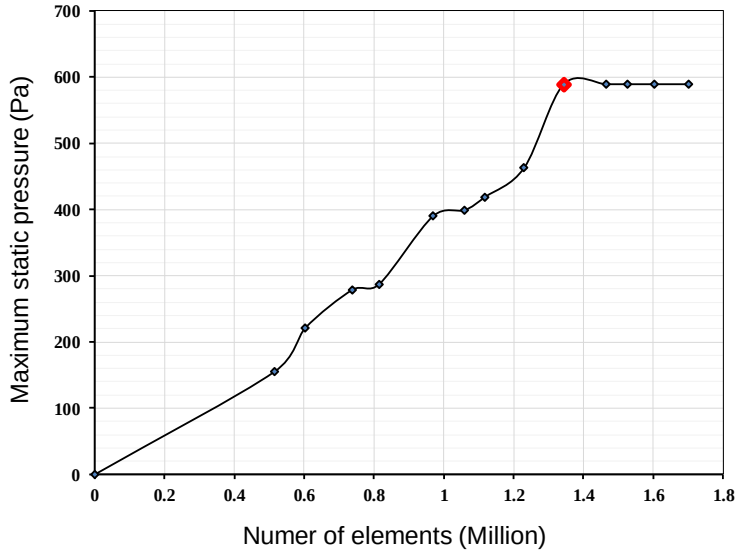

Fig. 3. Mesh sensitivity test

In order to capture the viscous effects associated to the developed boundary layer around the pantograph elements, mesh refinement was carried out around the pantograph as well as the wall boundaries as shown in Figure 4. In some of the specific applications, it is recommended to use discontinuous mesh approach for the turbulent flow [43-45].

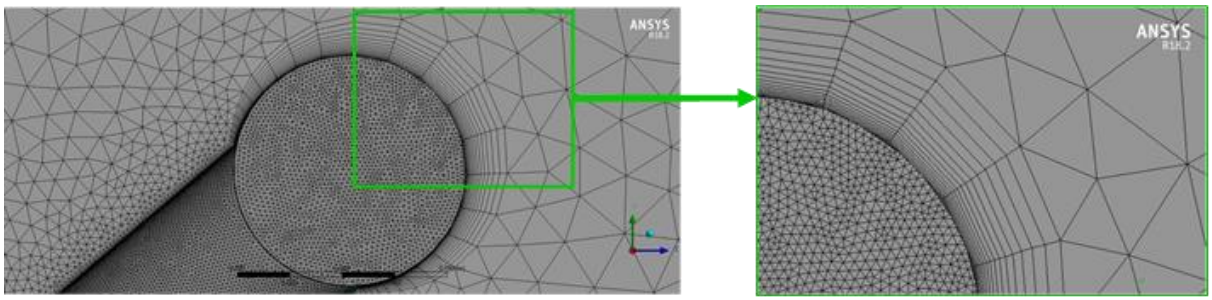

Fig. 4. Mesh refinement around the pantograph elements

3.2 Aerodynamic Simulation Criteria

To calculate the flow around the pantograph model, CFD analysis is usually used. However, Computational Aero-Acoustics (CAA) is used to numerically analyze the level of noise generated by the pantograph components [5]. The present computational simulations were carried out using FLUENT software package version 18.2. 3D flow field with pressure-based transient solver was used in the analysis to consider the vortex shedding. Realizable k-ε turbulence model was used in the simulations. The inlet and exit boundary conditions to the flow domain were set to be uniform velocity and uniform pressure gradient, respectively. External surface and object surface were

defined as cell zone condition. While standard wall function was used to define the boundary condition at the walls.

Usually, the value of the time step and number of time steps are selected based on the aero-acoustic requirements. For the present simulations, second-order implicit scheme was used with time step equals 2.5 × 10-4 s. While the number of time steps was set to 400. The computational simulations were carried out in ANSYS FLUENT software version 18.2. More information about all the flow governing equations for the developed model can be provided by the FLUENT user manual [30].

3.3 Acoustic Model

The literature survey of the aeroacoustics performance of the high-speed pantographs revealed that, the near-field and far-field sound pressure level of the pantograph can be determined by the application of the Acoustic Perturbation Equation (APE) and Ffowcs Williams and Hawkings (FW-H) approaches, respectively. Based on unsteady flow simulations, Ewert and Schröder [31] approach is applicable for the calculations of the near-field sound pressure calculations as it presents an explicit description of the acoustic level by solving the unsteady fluid flow simultaneously with the sound pressure in time domain [32]. Many approaches have been used to investigate the aerodynamic noise characteristics for the pantograph of high-speed trains. However, Ffowcs Williams-Hawkings (FW-H) equation was widely used to simulate the flow filed and the noise radiated from the far-field of the pantograph components [24,33-36]. In the present investigation, the aeroacoustics noise generated from the pantograph is then predicted by using FW-H approach. As the computational simulations of the generated noise from the pantograph of high-speed trains is extensive, this paper only focuses on the characteristics of far-field noise generated by the SSS87 articulated pantograph components.

The FW-H equation is derived by rearranging the exact Navier-Stokes and continuity equations. Integral techniques can be used for the wave propagation simulation to predict the noise signal from the far-field based on the inputs from near-filed. Although the solution of FW-H equation evolves both surface and volume integrals, the solution is usually approximated by only the surface integral [37]. In the simulations of aeroacoustics of high-speed trains, the FW-H method is often applied by integrating the surface that coinciding with the solid bodies such as the case in the pantograph. However, the method is also functional in the case where the surface is permeable and off the body. In the present investigation, all pantograph components are treated as impermeable surfaces for sound source in the FW-H approach. The sound is radiated from the sound source surfaces to the far-field point receivers. The FW-H equation can be expressed in the differential form as follows:

$$\left(\frac{\partial^2}{\partial t^2} - C_o^2 \frac{\partial^2}{\partial x_i \partial x_j}\right)(H(f)\acute{\rho}) = \frac{\partial^2}{\partial x_i \partial x_j}\left(T_{ij} H(f)\right) - \frac{\partial}{\partial x_i}\left(F_i \delta(f)\right) + \frac{\partial}{\partial t}\left(Q\delta(f)\right) \quad (1)$$

Where,

$$T_{ij} = \rho u_i v_j + P_{ij} - C_o^2 \acute{\rho} \delta_{ij} \quad (2)$$

$$F_i = \left(P_{ij} - \rho u_i (u_i - v_j)\right) \frac{\partial f}{\partial x_i} \quad (3)$$

$$Q = \left(\rho_o v_j + \rho(u_i - v_j)\right) \frac{\partial f}{\partial x_i} \quad (4)$$

The quadrupole sound source term in the right hand side of Eq. (1) is defined by the Lighthill stress tensor T_{ij}. The dipole term is defined the vector F_i, while the monopole conribution is denoted by Q that represents unsteady mass addition which can be ignored as the pantograph objects is considered as rigid bodies. The simulations was carried out at different train speeds of 300, 320 and 340 km/hr which corresponds to associated Mach numbers of 0.242, 0.242, 0.258 and 0.274, respectively. The ratio between the quadrupole to the dipole terms was found to be proportional to the square value of the associated Mach number [38]. The generated noise intensity of the quadrupole contribution is too small compared to the dipole source contribution as the pantograph is still running at subsonic low speeds [35]. The free stream conditions were denoted with the subscript "o", while the perturbation quantities are distinguished by the prime. The surfaces outside the desired solution region are defined by the function f=0 and $|\nabla f| = 1$. The Heavside function $H(f)$ is defined as follow:

$$\left.\begin{array}{ll} H(f) = 1 & \text{for } f > 0 \\ H(f) = 0 & \text{for } f < 0 \end{array}\right\} \quad (5)$$

The Dirac delta $\delta(f)$ presents the derivative of Heavside function $\acute{H}(f)$. While Kroneker delta in Eq. (2) is defined as follows:

$$\left.\begin{array}{ll} \delta_{ij} = 1 & \text{for } i = j \\ \delta_{ij} = 0 & \text{for } i \neq j \end{array}\right\} \quad (6)$$

P defines the pressure and the density is defined by ρ. u_i presents the fluid velocity at the surface normal direction and v_j is the moving body's velocity at the surface in normal direction. The Green function, is usually used for solving Eq. (1) in the time domain [39]. Another alternative approach can be used for solving FW-H equation in frequency domain, more details from the studies by Lockard [37,40].

4. Aerodynamic Flow Characteristics Around the Pantograph

The following sub-sections describe the simulation scenarios that were considered in the present work. For the validity of the obtained results, a comparison was made between the present results and those obtained by Siano *et al.,* [28] and Viscardi *et al.,* [29]. Then, the simulations were extended to study different models that were simulated to investigate the following parameters: (i) The effect of the pantograph speed on the flow field around the pantograph and the generated sound pressure level (SPL) at different operating conditions; (ii) The effect of modifying the panhead bars' cross-section on the generated acoustic pressure level.; (iii) The effect of the pantograph positioning on its aerodynamic performance.

4.1 Model Validation

For the validation of the present computational results, the setup of the present finite-volume model of the pantograph was adopted to the model proposed by Siano *et al.,* [28]. Thirty-five microphone receivers were placed at a distance of 1.0 m from the symmetry plane of the pantograph to replicate the experimental acoustic field measurements, Figure 5.

Figure 5 shows the computational microphone receivers' array, which was defined on Z and Y-axis. For Y-axis, the array was set from a maximum value equals to 0.8 m to a minimum value equals

to -0.8 m at intervals of 0.4 m. For Z-axis, the array was set from a maximum value equals to 1.2 m to a minimum value equals to -1.2 m at intervals of 0.4 m.

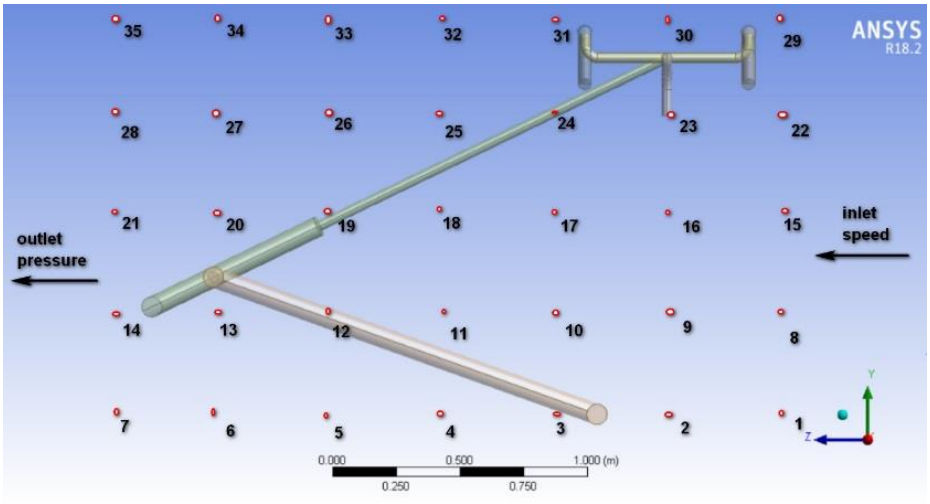

Fig. 5. Computational receivers array positions

Figure 6 represents a comparison between the present results and those obtained by Siano *et al.,* [28] for the acoustic pressure level at the pantograph. As shown in Figure 6, the signal contains a stationary and non-stationary part at a speed of 280 km/h. Measuring both transient and steady parts of the acoustic signal in one single measure is not recommended. The signal measured by the microphone receiver should be trimmed after almost 0.05 s to capture only the realistic acoustic noise of the transient part of the signal.

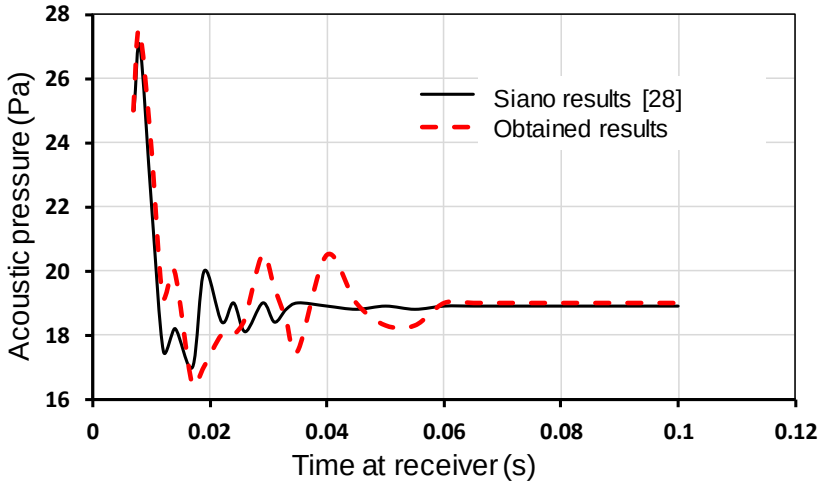

Fig. 6. Comparison of the obtained acoustic pressure and the reported experimental results of Siano *et al.,* [28] at train speed of 280 km/h

Small differences are noticed between the present results and those of Siano *et al.,* [28]. These differences may be attributed to the differences in the exported CAD model to the simulation environment, and the difference of the computational domain length. In the present model, a longer domain was considered to precisely capture the steady and transient flow fields around the pantograph.

4.2 Impact of Train Speed on The Pantograph Aeroacoustics Performance

The simulations were extended beyond the reported measurement of the SSS 87 pantograph to study the impact of train speed on the aerodynamic performance of the pantograph parts. Simulations for three models were carried out with different train speeds of 300 km/h (83.33 m/s), 320 km/h (88.89 m/s), and 340 km/h (94.44 m/s). The corresponding Mach numbers for the mentioned speeds were calculated to be 0.242, 0.258 and 0.274, respectively. Then the flow in all simulation scenarios is defined as incompressible subsonic flow. A very complex flow field including different size vortices was noticed in the wake as the pantograph mainly composed of rods. The instantaneous fluid flows around the pantograph at the symmetry plan can be seen in Figure 7 for a steady condition with train speed of 300 km/hr.

The turbulence model was able to accurately detect the vortex in the wake of the SSS87 pantograph. The pantograph frame is mainly composed of cylindrical bars. The dominant aerodynamic noise is then generated by the unsteady air flow around those cylindrical parts [41,42]. Strong unsteady flow separation was depicted in Figure 7 around the pantograph panhead and knee in accordance with the reported results by Lei *et al.,* [19]. The vortex shedding is the main source of the aerodynamic noise, which appears usually at commercial operating speeds of the high-speed trains. A dipole noise source is created due to the fluctuating forces created by vortices break up.

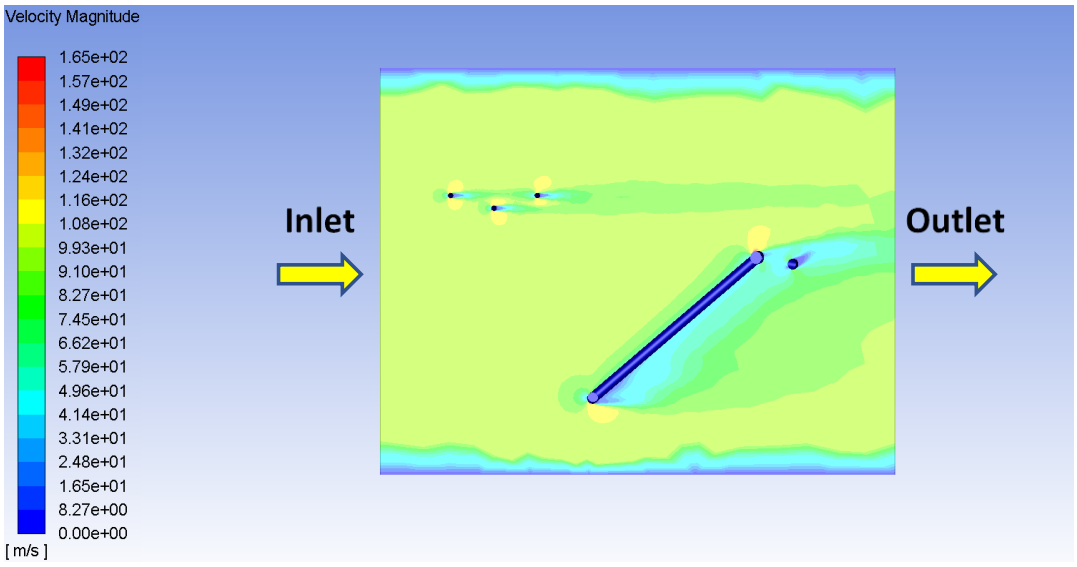

Fig. 7. Instantaneous computational velocity contours for train speeds of 300 km/h around the pantograph in the symmetry plan

It is worth mentioning that the vortex shedding phenomenon occurs due to something called the flow separation which occurs above a critical Reynolds number [42]. Due to the flow separation around the cylindrical surfaces of the pantograph, strong vortices can still be created and rapidly grow until they separate from the body.

The vortex shedding has a significant effect on the aeroacoustics noise at different velocities [16]. It was observed that the relationship between the vortex shedding and aeroacoustics noise is proportional. Figure 8 demonstrates the growth of vortex shedding around the cylindrical parts forming the pantograph panhead in the symmetry plan.

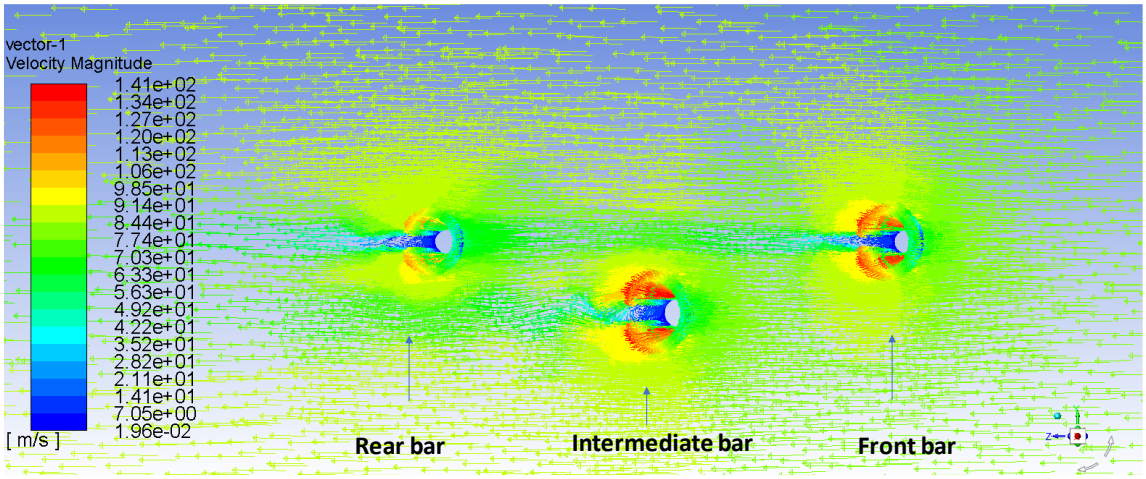

Fig. 8. Vortex shedding around cylindrical panhead bars of SSS 87 pantograph

Vortices appeared at the front cylindrical bar of the panhead and develops to collide with the vortices generated by the intermediate bar and finally hits the rear bar. This interaction between the vortices is very complex especially at high speeds. Strong flow separation appeared, and a complex flow wakes also appeared downstream due to the vortices produced from the interaction of the three cylindrical bars of the panhead. For this reason, some researchers have been working on optimising the space between the pantograph strips for aerodynamic noise reduction [50,51].

Figure 9 illustrates the contours of the total pressure around the pantograph. Given the development of the flow over time, it can be noted that, despite the uniform and steady entry conditions, the flow field evolves within the domain over time and this is due to the fact that turbulent flows are very unstable. In addition, given the transient model used, unfortunately after the first transient period of the time, the flow tends to become steady. The same behaviour is noticed for the total pressure, Figure 9.

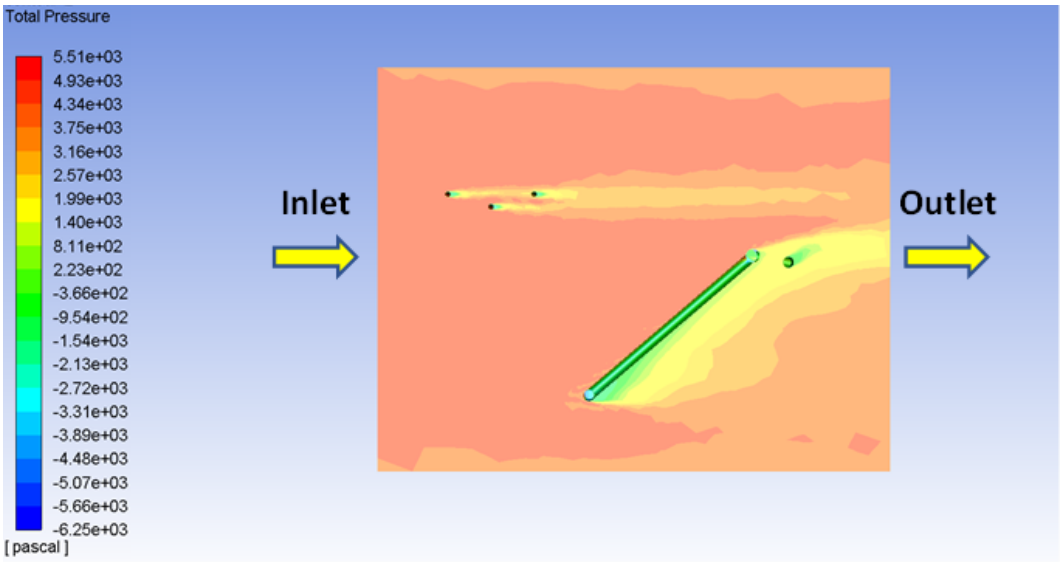

Fig. 9. Pressure contours around the tested pantograph model in the symmetry plan at train speeds of 300 km/h

Vortex shedding at the panhead not only produces an excitation with high frequencies that influence the aeroacoustics noise, but also has a strong influence on the quality of the power transmitted to the pantograph through the current collector. As a result, sparking may increase due

to the fluctuation of the produced drag and lifting forces as a result of the change in the pressure level at the bars of the pantograph panhead.

The increase in the train speed leads to increase in the wind speed around the pantograph, which leads to increase the acoustic pressure of the pantograph, especially at the cylindrical bars and pantograph knee. Figure 10 illustrates the variation of the acoustic pressure with time for the three different train speeds.

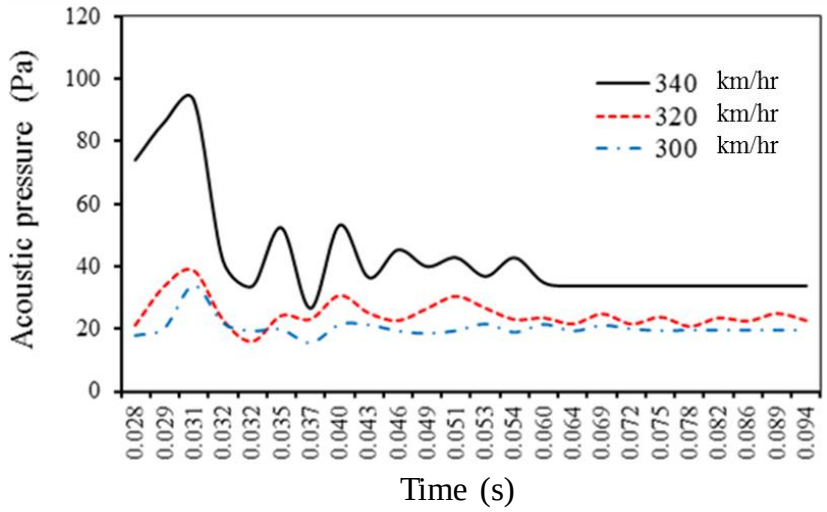

Fig. 10. Comparison of acoustic pressure measured at the pantograph panhead for the three different train speeds

Figure 10 depicts the variation of the acoustic pressure with the time for train speeds 300 km/h, 320 km/h, and 340 km/h. As can be seen in Figure 10, notable peeks of the acoustic pressure were detected at a speed of 340 km/h during the transient period. These peaks are associated to the shedding and vortices break up around the panhead cylindrical bars. While at speeds 300 km/h and 320 km/h the differences in the acoustic pressure levels are small.

4.3 Effect of Changing the Cross-Section of The Panhead Bars

Unlike the work presented by Siano *et al.,* [28], the present study considers the effect of the carbon layer on the top of the front and rear panhead cylindrical bars presenting the collector. The tested cross-sections in the present work are: Rounded edge; Figure 11(a), Elliptic edge; Figure 11(b), and Diamond edge; Figure 11(c). Schematics of the modified cross-sections used to simulate the pantograph panhead are depicted in Figure 11.

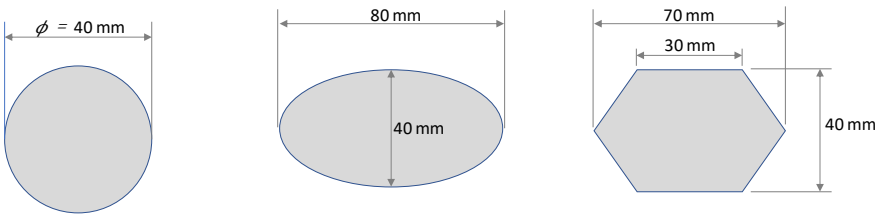

(a) Rounded Edge (b) Elliptic Edge (c) Diamond Edge

Fig. 11. Schematic definition of the cross-sections of the panhead front and rear bars

A comparison was made for the flow fields around the three sections used. The simulations were carried out on the same pantograph model at a uniform air speed of 83.3 m/s. As shown in Figure 12, the elliptic edge cross-section shows the lowest value for the air velocity, Figure 12(a), and the maximum total pressure, Figure 12(b), around the pantograph panhead.

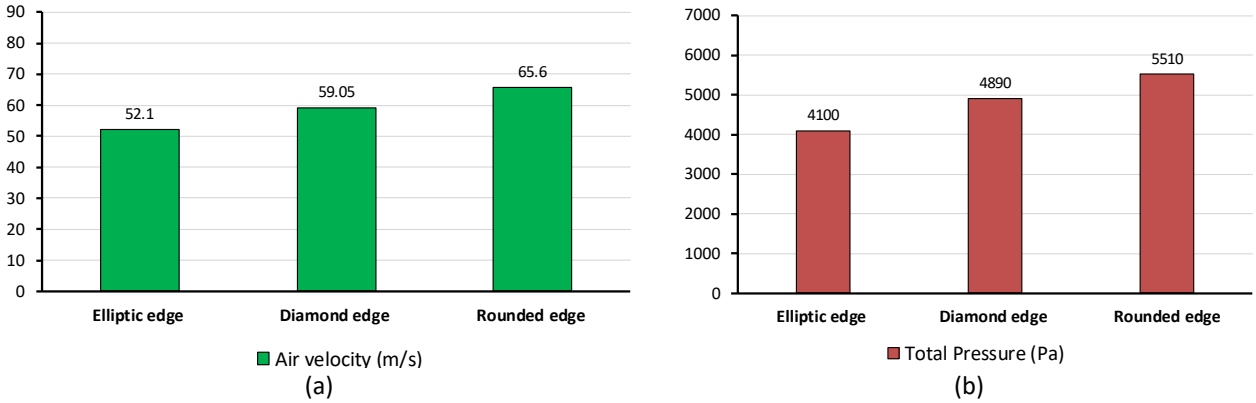

Fig. 12. Comparison between the three different shapes of the pantograph panhead bars' cross-section

From the comparison, it can be concluded that the fluctuating forces produced from the flow separation around the elliptic-edge is low in comparison to the diamond- and the rounded-edge cross-sections as seen in Figure 12. Thus, the aerodynamic noise that is associated with the vortex shedding is reduced. Moreover, the acoustic pressure level is decreased as it can be seen in Figure 13. Using the Elliptic-edge also reduces the fluctuation in the lifting forces on the pantograph leading-edge for better performance with reduction in the probability of sparking.

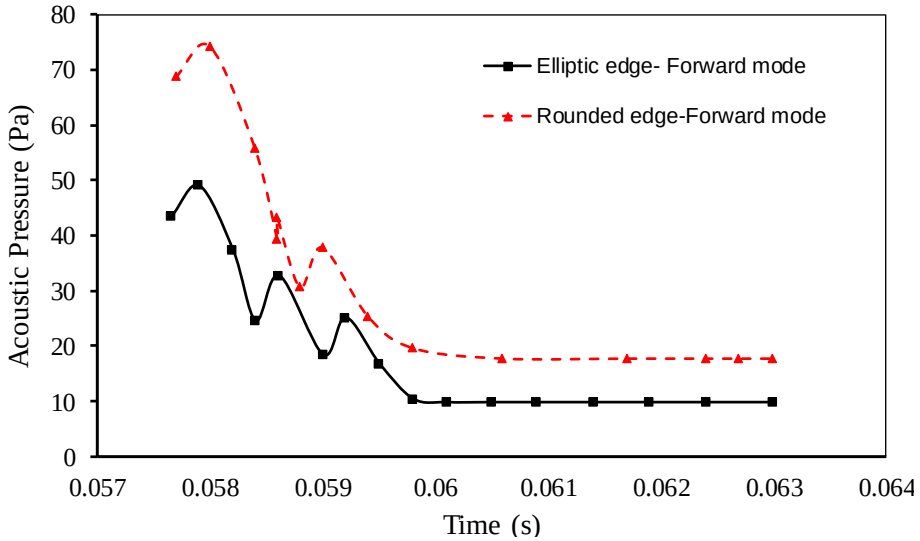

Fig. 13. CFD results of the acoustic pressure vs. time at the receiver for the panhead with elliptic-edge and rounded edge cross-section at train speed of 250 km/h

Further aerodynamic noise analysis was performed for the pantograph panhead section as it represents the dominant source of the detected noise. A comparison was made for the panhead with rounded edge and elliptic-edge sections in different running speeds. As the panhead with the diamond-edge section exhibited the highest level of the acoustic pressure, it was excluded from the

comparison. The models were simulated at two uniform inlet velocities of 69.44 m/s and 83.33 m/s in both forward- and reverse-movement modes.

Figure 14 shows the comparison of the results of the different models at velocity of 69.44 m/s in both forward and reverse movement modes. Notable differences were detected in the acoustic pressure during the transient period. In the steady period, the model with the elliptic-edge in forward mode had the lowest acoustic pressure-level, while only very small differences were detected for the rounded-edge section in both the reverse and forward modes.

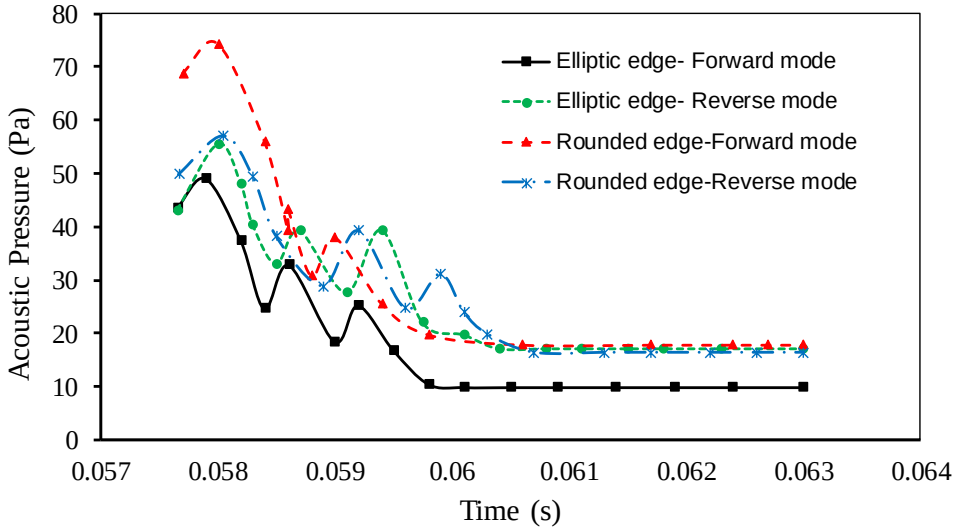

Fig. 14. CFD results of the acoustic pressure vs. time at receiver at inlet velocity of 69.44 m/s (train speed of 250 km/h)

5. Conclusions

One of the major sources of noise for high-speed trains is the pantograph aerodynamic noise. At high operating speeds above 300 km/h, the aerodynamic noise grows to be comparable to the rolling contact noise. To reduce pantograph noise, it is necessary to understand the noise creation mechanism for a pantograph. However, it is difficult to estimate this mechanism due to the complexity of the pantograph components. By using computational modelling, it is possible to detect the portion of the pantograph that generates the highest level of noise. For these reasons, the advanced aerodynamic noise prediction using computational simulations is accurate, reliable, and efficient. The present paper introduces a computational model for the assessment of the aerodynamic noise from high speed pantograph. The obtained results from the computational simulations were verified against the computational and experimental measurements in the literature for the same pantograph model. The simulations were carried out on the pantograph using different train running speeds. It was found that the vortex shedding at the pantograph's panhead was the dominant source of noise. Large flow separation was detected at the cylindrical bars forming the panhead, which leads to the acoustic pressure fluctuations at the panhead.

Different designs for the pantograph's panhead front and rear bars were suggested to reduce the aerodynamic noise generated at the panhead part. Based on the obtained computational results, it was found that the use of an elliptic-edge cross-section bars can be a potential modification in the collector shape that can reduce the aerodynamic noise at the panhead for speeds up to 250 km/h. For higher velocities up to 340 km/h, the elliptic edge sections can also be used as a potential solution for reducing the possibility of sparking. It was noticed that the highest level of aerodynamic noise was detected at the pantographs' panhead, knee and coupling rode. Further investigations are still

needed to optimize the dimensions of the carbon strips with the positioning and geometry modifications of the cylindrical bars forming the panhead.

References

[1] Schulte-Werning, Burkhard, David Thompson, Pierre-Etienne Gautier, Carl Hanson, Brian Hemsworth, James Nelson, Tatsuo Maeda, and Paul de Vos, eds. *Noise and vibration mitigation for rail transportation systems: proceedings of the 9th International Workshop on Railway Noise*, Munich, Germany, 4-8 September 2007. Vol. 99. Springer Science & Business Media, 2008.

[2] Thompson, David. *Railway noise and vibration: mechanisms, modelling and means of control*. Elsevier, 2008.

[3] Zhang, Xuetao. "Empirical modeling of railway aerodynamic noise using one microphone pass-by recording." In *Noise and Vibration Mitigation for Rail Transportation Systems*, pp. 125-131. Springer, Berlin, Heidelberg, 2015. https://doi.org/10.1007/978-3-662-44832-8_17

[4] He, B., X. Xiao, X. Zhou, J. Han, and X. Jin. "Characteristics of sound insulation and insertion loss of different deloading sound barriers for high-speed railways." In *Noise and Vibration Mitigation for Rail Transportation Systems*, pp. 345-352. Springer, Berlin, Heidelberg, 2015. https://doi.org/10.1007/978-3-662-44832-8_41

[5] Poisson, F. "Railway noise generated by high-speed trains." In *Noise and Vibration Mitigation for Rail Transportation Systems*, pp. 457-480. Springer, Berlin, Heidelberg, 2015. https://doi.org/10.1007/978-3-662-44832-8_55

[6] Galuba, Judith, and Carsten Spehr. "Concept for Measuring Aeroacoustic Noise Transmission in Trains Derived from Experience Gained in Aircraft Testing." In *Noise and Vibration Mitigation for Rail Transportation Systems*, pp. 165-172. Springer, Berlin, Heidelberg, 2015. https://doi.org/10.1007/978-3-662-44832-8_22

[7] Kurita, Takeshi, Masaaki Hara, Haruo Yamada, Yuusuke Wakabayashi, Fumio Mizushima, Hitoshi Satoh, and Toshio Shikama. "Reduction of pantograph noise of high-speed trains." *Journal of Mechanical systems for Transportation and Logistics* 3, no. 1 (2010): 63-74. https://doi.org/10.1299/jmtl.3.63

[8] Mitsumoji, T., T. Sueki, N. Yamazaki, Y. Sato, M. Ikeda, R. Takinami, H. Gejima, and Koji Fukagata. "Aerodynamic noise reduction of a pantograph panhead by applying a flow control method." In *Noise and Vibration Mitigation for Rail Transportation Systems*, pp. 515-522. Springer, Berlin, Heidelberg, 2015. https://doi.org/10.1007/978-3-662-44832-8_60

[9] Noger, C., J. C. Patrat, J. Peube, and J. L. Peube. "Aeroacoustical study of the TGV pantograph recess." *Journal of Sound and Vibration* 231, no. 3 (2000): 563-575. https://doi.org/10.1006/jsvi.1999.2545

[10] Nagakura, Kiyoshi. "Localization of aerodynamic noise sources of Shinkansen trains." *Journal of Sound and Vibration* 293, no. 3-5 (2006): 547-556. https://doi.org/10.1016/j.jsv.2005.08.043

[11] Lee, Yeongbin, Joohyun Rho, Minho Kwak, Jaeho Lee, Kyuhong Kim, and Dongho Lee. "Aerodynamic characteristics of high speed train pantograph with the optimized panhead shape." In *International Conference on FLUID MECHANICS and Aerodynamics*. 2009.

[12] Lölgen, Thomas. "Wind tunnel noise measurements on full-scale pantograph models." *The Journal of the Acoustical Society of America* 105, no. 2 (1999): 1136. https://doi.org/10.1121/1.425410

[13] Guo-Hua, Cai. "The experimental technique of pantograph of super express train in low speed wind tunnel." *Journal of Railway Engineering Society* 4 (2006): 67-70.

[14] Lauterbach, Andreas, Klaus Ehrenfried, Sigfried Loose, and Claus Wagner. "Microphone array wind tunnel measurements of Reynolds number effects in high-speed train aeroacoustics." *International Journal of Aeroacoustics* 11, no. 3-4 (2012): 411-446. https://doi.org/10.1260/1475-472X.11.3-4.411

[15] K. Manabe, T.M., and T. Okubo. "The aerodynamic sound from pantograph and the reducing method (1) - Wind tunnel tests on the existing pantograph." *Railway Technical Research Report* 1237 (1983): 655-671.

[16] Noh, Hee-Min. "Wind tunnel test analysis to determine pantograph noise contribution on a high-speed train." *Advances in Mechanical Engineering* 11, no. 10 (2019): 1687814019884778. https://doi.org/10.1177/1687814019884778

[17] Ikeda, Mitsuru, and Takeshi Mitsumoji. "Evaluation method of low-frequency aeroacoustic noise source structure generated by Shinkansen pantograph." *Quarterly Report of RTRI* 49, no. 3 (2008): 184-190. https://doi.org/10.2219/rtriqr.49.184

[18] Ikeda, Mitsuru, and Takeshi Mitsumoji. "Numerical estimation of aerodynamic interference between panhead and articulated frame." *Quarterly Report of RTRI* 50, no. 4 (2009): 227-232. https://doi.org/10.2219/rtriqr.50.227

[19] Lei, Shi, Zhang Chengchun, Wang Jing, and Ren Luquan. "Numerical analysis of aerodynamic noise of a high-speed pantograph." In *2013 Fourth International Conference on Digital Manufacturing & Automation*, pp. 837-841. IEEE, 2013. https://doi.org/10.1109/ICDMA.2013.19 8

[20] Iglesias, E. Latorre, D. J. Thompson, and M. G. Smith. "Component-based model to predict aerodynamic noise from high-speed train pantographs." *Journal of Sound and Vibration* 394 (2017): 280-305. https://doi.org/10.1016/j.jsv.2017.01.028

[21] Behr, W., T. Lolgen, W. Baldauf, L. Willenbrink, R. Blaschko, K. Jager, and J. Kremlacek. "Low noise pantograph ASP-recent developments." In *INTERNOISE 2000. PROCEEDINGS OF THE 29TH INTERNATIONAL CONGRESS ON NOISE CONTROL ENGINEERING*, HELD 27-31 AUGUST 2000, NICE, FRANCE., vol. 4. 2000. https://doi.org/10.1260/0957456001498057

[22] Baldauf, Wilhelm, Rene Blaschko, Wolfgang Behr, Christoph Heine, and Michael Kolbe. "Development of an actively controlled, acoustically optimised single arm pantograph." In *Proceedings of the World Congress of Railway Research WCRR*. 2001.

[23] Ikeda, Mitsuru, Takeshi Mitsumoji, Takeshi Sueki, and Takehisa Takaishi. "Aerodynamic noise reduction in pantographs by shape-smoothing of the panhead and its support and by use of porous material in surface coverings." *Quarterly Report of RTRI* 51, no. 4 (2010): 220-226. https://doi.org/10.2219/rtriqr.51.220

[24] Xiao-Ming, Tan, Yang Zhi-Gang, Tan Xi-ming, Wu Xiao-long, and Zhang Jie. "Vortex structures and aeroacoustic performance of the flow field of the pantograph." *Journal of Sound and Vibration* 432 (2018): 17-32. https://doi.org/10.1016/j.jsv.2018.06.025

[25] Bruni, Stefano, Jorge Ambrosio, Alberto Carnicero, Yong Hyeon Cho, Lars Finner, Mitsuru Ikeda, Sam Young Kwon et al. "The results of the pantograph-catenary interaction benchmark." *Vehicle System Dynamics* 53, no. 3 (2015): 412-435. https://doi.org/10.1080/00423114.2014.953183

[26] Pombo, Joao, J. Ambrósio, M. Pereira, F. Rauter, Andrea Collina, and Alan Facchinetti. "Influence of the aerodynamic forces on the pantograph-catenary system for high-speed trains." *Vehicle System Dynamics* 47, no. 11 (2009): 1327-1347. https://doi.org/10.1080/00423110802613402

[27] Ambrósio, Jorge, Joao Pombo, and Manuel Pereira. "Optimization of high-speed railway pantographs for improving pantograph-catenary contact." *Theoretical and Applied Mechanics Letters* 3, no. 1 (2013): 013006. https://doi.org/10.1063/2.1301306

[28] Siano, D., M. Viscardi, F. Donisi, and P. Napolitano. "Numerical modeling and experimental evaluation of an high-speed train pantograph aerodynamic noise." *Computers and Mathematics in Automation and Materials Science* 12, no. 1 (2011): 86-92.

[29] Viscardi, M., D. Siano, P. Napolitano, and F. Donisi. "An analytical model for the aerodynamic noise prediction of an high-speed train pantograph." *Applied Informatics and Communications* (2014): 271-280.

[30] ANSYS. "Fluent user's guide. Release 18.2." *ANSYS, Inc*. (2017).

[31] Ewert, Roland, and Wolfgang Schröder. "Acoustic perturbation equations based on flow decomposition via source filtering." *Journal of Computational Physics* 188, no. 2 (2003): 365-398. https://doi.org/10.1016/S0021-9991(03)00168-2

[32] Ewert, R., and W. Schröder. "On the simulation of trailing edge noise with a hybrid LES/APE method." *Journal of Sound and Vibration* 270, no. 3 (2004): 509-524. https://doi.org/10.1016/j.jsv.2003.09.047

[33] Williams, JE Ffowcs, and David L. Hawkings. "Sound generation by turbulence and surfaces in arbitrary motion." *Philosophical Transactions for the Royal Society of London. Series A, Mathematical and Physical Sciences* (1969): 321-342. https://doi.org/10.1098/rsta.1969.0031

[34] Yu, Hua-Hua, Jia-Chun Li, and Hui-Qin Zhang. "On aerodynamic noises radiated by the pantograph system of high-speed trains." *Acta Mechanica Sinica* 29, no. 3 (2013): 399-410. https://doi.org/10.1007/s10409-013-0028-z

[35] Zhang, YaDong, JiYe Zhang, Tian Li, and Liang Zhang. "Investigation of the aeroacoustic behavior and aerodynamic noise of a high-speed train pantograph." *Science China Technological Sciences* 60, no. 4 (2017): 561-575. https://doi.org/10.1007/s11431-016-0649-6

[36] Yao, Yongfang, Zhenxu Sun, Guowei Yang, Wen Liu, and Prasert Prapamonthon. "Analysis of aerodynamic noise characteristics of high-speed train pantograph with different installation bases." *Applied Sciences* 9, no. 11 (2019): 2332. https://doi.org/10.3390/app9112332

[37] Lockard, David. "A comparison of Ffowcs Williams-Hawkings solvers for airframe noise applications." In *8th AIAA/CEAS Aeroacoustics Conference & Exhibit*, p. 2580. 2002. https://doi.org/10.2514/6.2002-2580

[38] Li, Tian, Deng Qin, Weihua Zhang, and Jiye Zhang. "Study on the aerodynamic noise characteristics of high-speed pantographs with different strip spacings." *Journal of Wind Engineering and Industrial Aerodynamics* 202 (2020): 104191. https://doi.org/10.1016/j.jweia.2020.104191

[39] Crighton, David George, Ann P. Dowling, J. E. Ffowcs-Williams, Manfred Heckl, F. G. Leppington, and James F. Bartram. "Modern Methods in Analytical Acoustics Lecture Notes." *Acoustical Society of America Journal* 92, no. 5 (1992): 3023. https://doi.org/10.1121/1.404334

[40] Lockard, David P. "An efficient, two-dimensional implementation of the Ffowcs Williams and Hawkings equation." *Journal of Sound and Vibration* 229, no. 4 (2000): 897-911. https://doi.org/10.1006/jsvi.1999.2522

[41] Blevins, R. D. "The effect of sound on vortex shedding from cylinders." *Journal of Fluid Mechanics* 161 (1985): 217-237. https://doi.org/10.1017/S0022112085002890
[42] Williamson, Charles HK. "Oblique and parallel modes of vortex shedding in the wake of a circular cylinder at low Reynolds numbers." *Journal of Fluid Mechanics* 206 (1989): 579-627. https://doi.org/10.1017/S0022112089002429
[43] Ahmad, Nor Elyana, Essam Abo-Serie, and Adrian Gaylard. "Mesh optimization for ground vehicle aerodynamics." *CFD Letters* 2, no. 1 (2010): 54-65.
[44] Alfarawi, Suliman, Azeldin El-sawi, and Hossin Omar. "Exploring Discontinuous Meshing for CFD Modelling of Counter Flow Heat Exchanger." *Journal of Advanced Research in Numerical Heat Transfer* 5, no. 1 (2021): 26-34.
[45] Samion, Siti Ruhliah Lizarose, and Mohamed Sukri Mat Ali. "Aerodynamic noise measurement in anechoic wind tunnel of rod-airfoil with leading edge serrations." *Journal of Advanced Research in Fluid Mechanics and Thermal Sciences* 47, no. 1 (2018): 97-107.
[46] Kim, Hogun, Zhiwei Hu, and David Thompson. "Effect of different typical high speed train pantograph recess configurations on aerodynamic noise." *Proceedings of the Institution of Mechanical Engineers, Part F: Journal of Rail and Rapid Transit* 235, no. 5 (2021): 573-585. https://doi.org/10.1177/0954409720947516
[47] Toward, Martin, and Daniel Lurcock. "Comparisons of Aerodynamic Noise Results Between Computations and Experiments for a High-Speed Train Pantograph." In *Noise and Vibration Mitigation for Rail Transportation Systems: Proceedings of the 13th International Workshop on Railway Noise*, 16-20 September 2019, Ghent, Belgium, p. 66. Springer Nature, 2021. https://doi.org/10.1007/978-3-030-70289-2_4
[48] Saito, Mitsuru, Fumio Mizushima, Yusuke Wakabayashi, Takeshi Kurita, Shinji Nakajima, and Toru Hirasawa. "Development of New Low-Noise Pantograph for High-Speed Trains." In *Noise and Vibration Mitigation for Rail Transportation Systems*, pp. 81-89. Springer, Cham, 2021. https://doi.org/10.1007/978-3-030-70289-2_6
[49] Xiao, Chenghuan, Mingzhi Yang, Changda Tan, and Zhaijun Lu. "Effects of platform sinking height on the unsteady aerodynamic performance of high-speed train pantograph." *Journal of Wind Engineering and Industrial Aerodynamics* 204 (2020): 104284. https://doi.org/10.1016/j.jweia.2020.104284
[50] Dai, Zhiyuan, Tian Li, Jian Deng, Ning Zhou, and Weihua Zhang. "Effect of the strip spacing on the aerodynamic performance of a high-speed double-strip pantograph." *Vehicle System Dynamics* (2021): 1-17. https://doi.org/10.1080/00423114.2021.1945117
[51] Li, Tian, Deng Qin, Weihua Zhang, and Jiye Zhang. "Study on the aerodynamic noise characteristics of high-speed pantographs with different strip spacings." *Journal of Wind Engineering and Industrial Aerodynamics* 202 (2020): 104191. https://doi.org/10.1016/j.jweia.2020.104191